Study of the scientific performances and calibration of the Athena's X-ray Integral Field Unit

Florent Castellani

Supervisors: François Pajot , Etienne Pointecouteau

irap astrophysique & planétologie

cnes CENTRE NATIONAL D'ÉTUDES SPATIALES

Abstract : The X-ray Integral Field Unit (X-IFU) on-board the Athena mission is a cryogenic x-ray spectrometer operating at 90 mK. With its pixel array of 3168 Transition Edge Sensors (TES), it will provide unprecedented spatially resolved high-resolution spectroscopy (2.5 eV FWHM up to 7 keV) in the 0.2-12 keV energy range. The X-IFU is at the end of its preliminary definition Phase (Phase B). In this context, we need to test and assess the capabilities of the X-IFU. Realistic mock observations and functional demonstration of the detection chain are key tools to demonstrate that the X-IFU complies to the specific science requirements. In this view I present my results and work perspectives for: 1) The test of the electronic readout chain integrated in the CNES/IRAP cryogenic test bench. 2) End-to-end simulations of the X-IFU observations for a distant group of galaxies.

Athena's X-ray Integral Field Unit

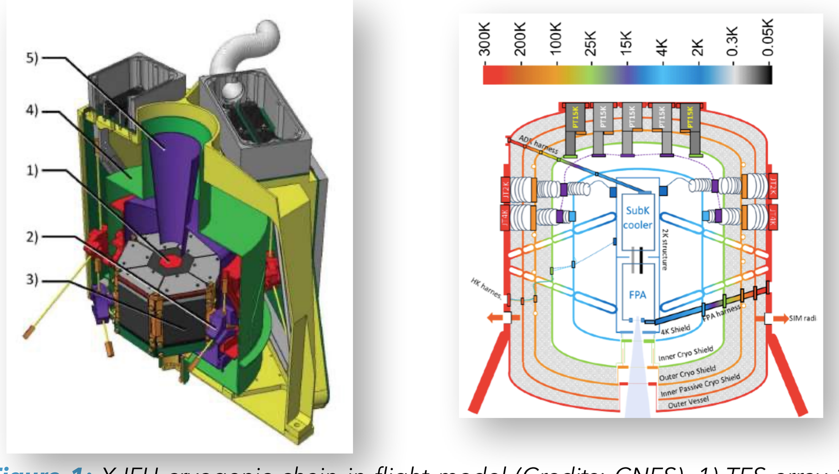

Figure 1: X-IFU cryogenic chain in flight model (Credits: CNES). 1) TES array 2) Kevlar suspension 3) Readout assembly with FE SQUID chip 4) Mu-metal shield 5) Nb shield

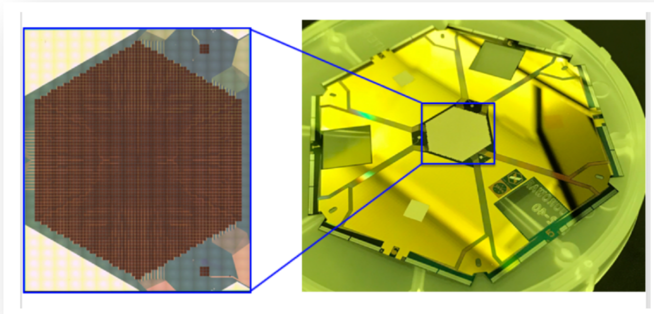

Figure 2: Prototype TES microcalorimeter array (left) and its supporting wafer (right) (Credits: NASA/GSFC)

- Athena is the ESA L2 mission dedicated to the study of the Hot and Energetic universe [1]
  - How does ordinary matter assemble to create the large scale structures?
  - How do black holes grow and shape their surrounding Universe?
- The X-IFU is built by a consortium of 11 European countries with contributions from the USA and Japan (PI-ship: IRAP, Prime: CNES)
- It is a cryogenic imaging spectrometer operating at 90mK, its key performance requirements are listed in Table 1.

Spectral resolution	2.5 eV (E < 7 keV)
Field of view	5' (equivalent diameter)
Angular resolution	~ 5" (~mirror PSF HEW)
Background level	<5 10^{-3} count/s/cm²/keV
Energy range	0.2 - 12 keV
Gain calibration error	0.4 eV
Count rate capability	1 mCrab (2.5 eV, 80% eff.) 10 mCrab (2.5 eV, 80% eff.,goal) 1 Crab (<30 eV, 30% eff.)

Table 1: High level performance parameters of the X-IFU (see also [2])

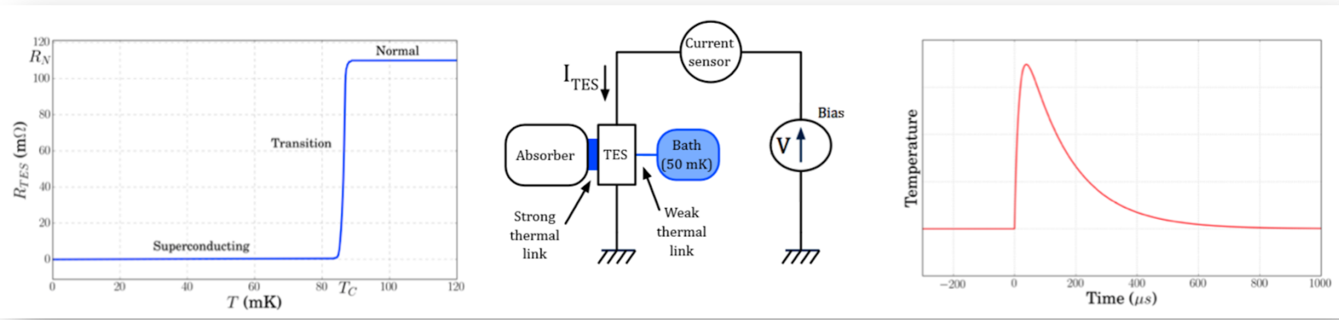

Figure 3: Illustration of the TES detection principle. Left: superconducting transition of TES. Middle: schematic of electro-thermal circuit of TES. Right: Plot of temperature during photon detection [3].

Objectives

- The evaluation of the feasibility of the objectives for the Hot Universe core science of X-IFU/Athena with respect to the anticipated performances of the instrument.
  - Testing and validating X-IFU capabilities together with end-to-end numerical simulations and functional test bench
- Development of new processing tools for the X-IFU high spectral resolution data.
  - Developing post-processing tools to take advantage of the spectral high-resolution
- Functional demonstration of the detection chain of the X-IFU using the cryogenic test bench at IRAP.
  - Undertaking an end-to-end demonstration of the cryogenic detection chain of X-ray photons for further implementation and calibration

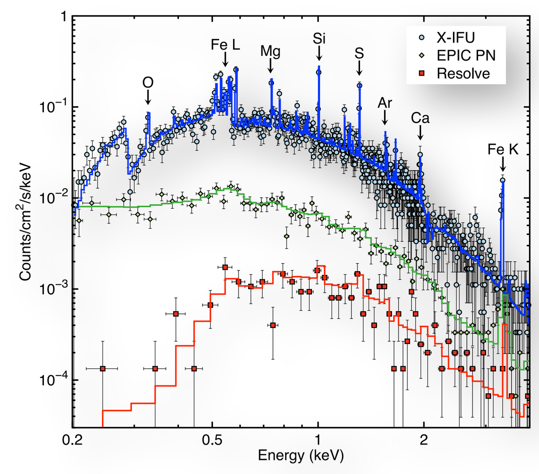

Figure 4: Simulated X-IFU spectrum at z=1 of a galaxy cluster with kT =3 keV [1]

50mK Test Bench at IRAP

- In order to test and validate the cryogenic TES detection chain, a CNES/IRAP Test Bench (named Elsa) has been developed to perform a functional demonstration of the detection chain.
- That includes the cryogenic readout sub-system plugged on TES as well as the warm readout chain: the WFEE (Warm Front End Electronics [4] and the DRE (Digital Readout Electronics [3]).
- The 50 mK stage is provided by a multi-stage cryostat from Entropy GmbH made up of:
  - A two-stage pulse tube cooler reaching 70K and 4K.
  - An ADR (Adiabatic Demagnetisation Refrigerator) composed by superconducting magnet and a salt pill unit delivering ~35mK base temperature.

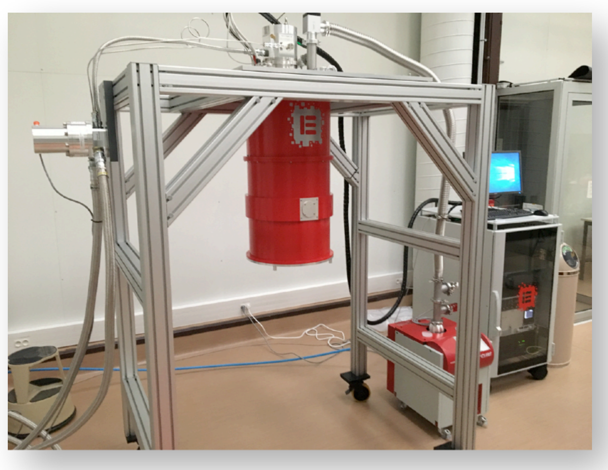

Figure 5: Elsa test bench ADR cryostat in the IRAP high bay clean room

Figure 6: The 50mK plate equipped with thermometers and an sample heater for heat load tests

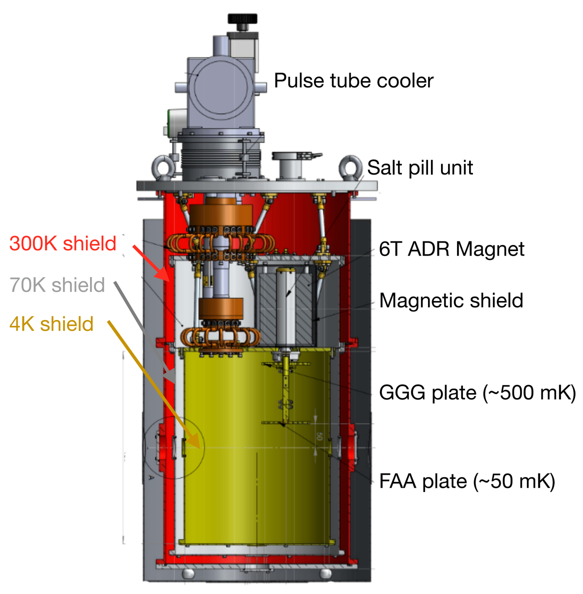

Figure 7: Schematic of the test bench cryostat

Cryostat Characterisation and Build-up

- Before implementing the TES and electronic readout chain, it is important to characterise the 50mK test bench cryostat performances:
  - Magnetic (residual) field inside the cryostat has been measured to acceptable result (i.e. <1 μT)
  - The level of micro-vibrations transmitted by the ground floor has been assessed (Figure 9) and reduced with shock absorbers.
  - Nominal temperature stability has been verified, with a standard deviation of 3 μK at 50mK.
  - Heat load tests (1 μW) have been performed in order to study the ADR magnet behaviour (Figure 8).
- The test bench will then be implemented with:
  - A NASA/GSFC 2x32 TES pixel array installed at the focal plane
  - Visible/IR blocking filters along the optical path
  - A radioactive Fe-55 as a source of X-ray photons at the energy of E = 6.4 keV
  - Laboratory room temperature readout electronics by NASA/GSFC, to be later replaced by the baseline WFEE from APC and DRE from IRAP.

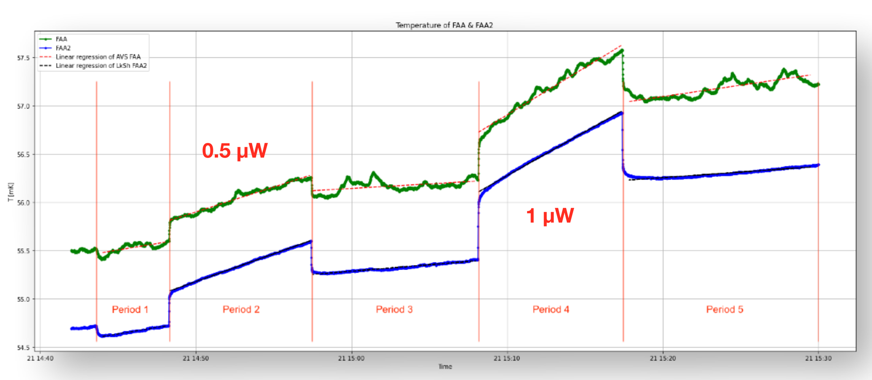

Figure 8: Plot of thermometry measurements at two different parts of the 50mK plate. The five periods correspond to several heat loads with sample heater: periods 1,3 and 5 corresponds to no heat load while period 2: 0.5μW and period 4: 1μW. Measurements of step heights allowed to compute the thermal conductance of the salt pill unit "cold finger" (G = 4 ± 2 μW/mK corresponding to RRR = 60 ± 30).

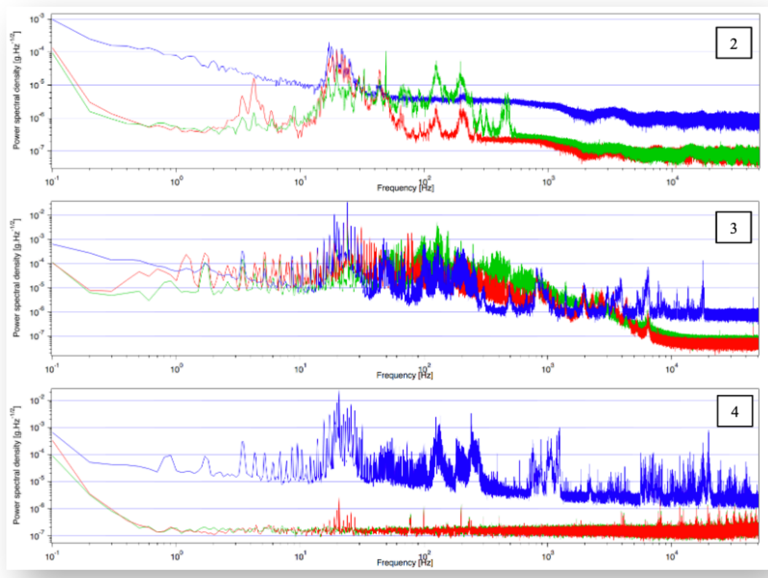

Figure 9: Measured power spectral density of micro-vibration signals on the 3 different axes: x (blue) for left and right, y (red) for front and back, z (green) for up and down. The x-axis probe is a cryogenic sensor and so more sensitive than the others.

X-IFU end-to-end Simulator

- To study the scientific performances of X-IFU, the end-to-end SIXTE simulator has been developed to produce an X-IFU event list of a simulated X-ray source.
- This simulator takes into account:
  - Properties of the sources like geometry, timing variation, spectra,…
  - Detector geometry (pixel size)
  - Full imaging process (PSF, vignetting,…)
  - Instrumental effects (background, cross-talks, …)

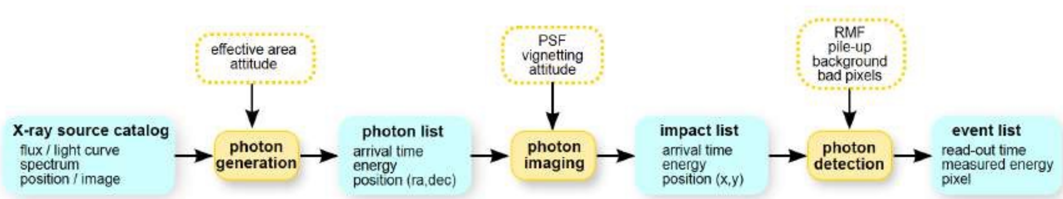

Figure 10: Data flow of the end-to-end SIXTE pipeline from [5]

- The output simulated observation may be post-processed with imaging and spectral analysis tools in order to perform scientific research.

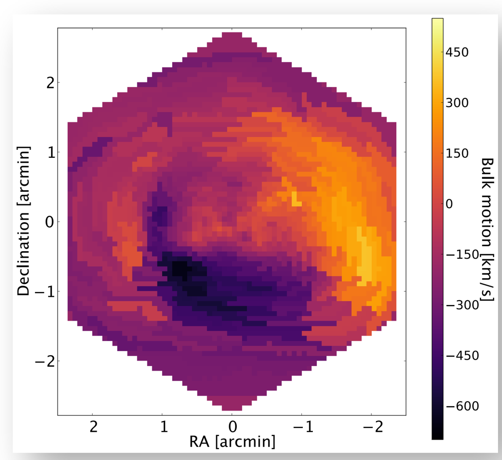

Figure 11: Reconstructed bulk motion velocity field of the hot intra-cluster gas for a 50 ks X-IFU observation [6]

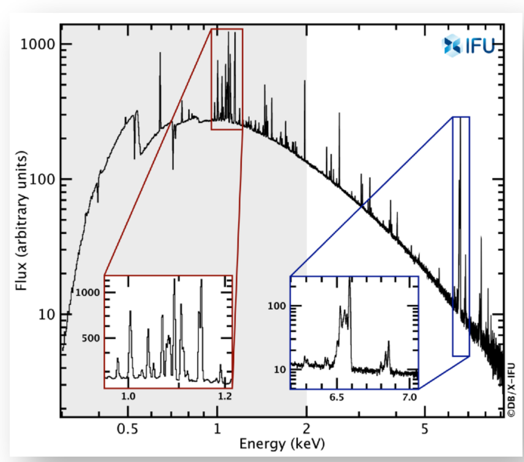

Figure 12: Perseus spectrum seen by the X-IFU simulated for a 100 ks exposure time [7]

Show-case of X-IFU capabilities

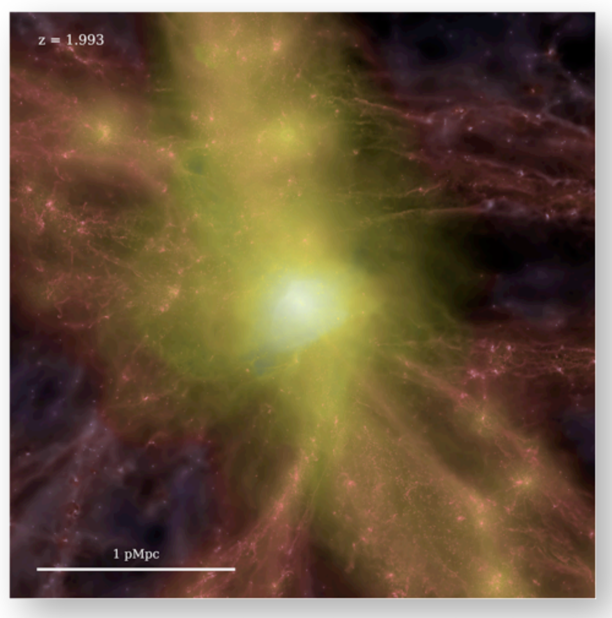

Figure 13: Gas particles visualisation on the selected group of galaxies in cosmological simulations. (Credits: Yannick Bahé/Hydrangea Team)

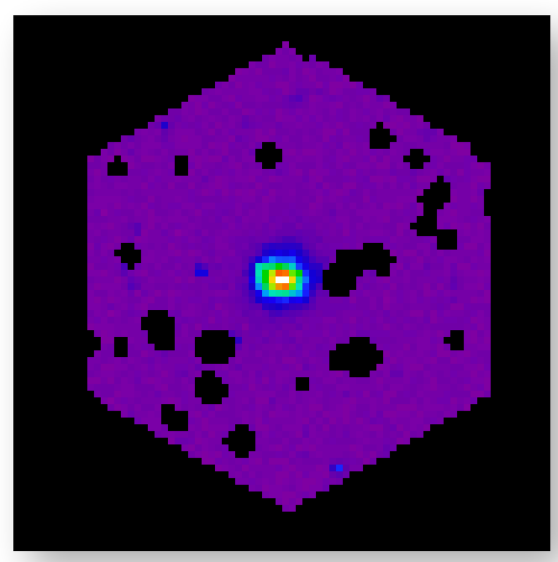

Figure 14: Count image simulated by SIXTE. Astrophysical, Cosmic and Non-X-ray background have been simulated following the same methodology as [6]. Resolved AGN background has been removed.

- Demonstrate the abilities of X-IFU to perform a physical characterisation of early group and clusters.
- Mock observations of a distant (z = 2) group of galaxies (M_{500} = 7 10^{13} M_{sun}/h) extracted from HYDRANGEA cosmological SPH simulation [8].
- Input to X-IFU simulations:
  - Bulk motion velocity of the ICM (Intra Cluster Medium) like in Figure 11
  - Chemical abundances of the ICM and spatial distribution of those chemical species into the cluster.
  - Dynamical structure of the cluster (such as merger groups,…)
- In order to recover the galaxy cluster physical characteristics I develop post-processing tools to be used later on X-IFU nominal utilisation.

References:

[1] Barret et al., 2016, Proceedings SPIE, Vol 9905, 99052F
[2] Pajot et al., 2018, 2018, JLTP 193, 901
[3] Ravera et al., 2018, Proceedings SPIE, Vol 10699,106994V
[4] Chen et al., 2018, Proceedings SPIE, Vol 10699, 106994P
[5] Dauser et al., 2019, A&A, Vol 630
[6] Cucchetti et al., 2018, A&A, Vol 620
[7] Barret et al., 2018, Proceedings SPIE, Vol 10699, 106991G
[8] Bahé et al., 2017, MNRAS, Vol 470

ATHENA X-IFU X-ray Integral Field Unit